

Kinetics of hydroformylation of styrene using homogeneous rhodium complex catalyst

Vinod S. Nair, Suju P. Mathew, Raghunath V. Chaudhari *

Homogeneous Catalysis Division, National Chemical Laboratory, Pune, India

Received 6 June 1998; accepted 7 October 1998

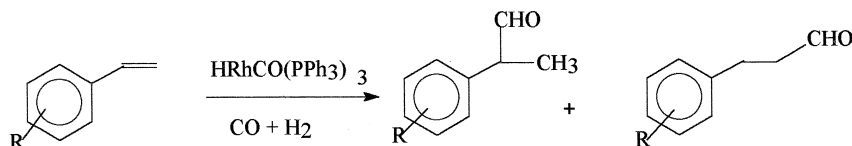
Abstract

The kinetics of hydroformylation of styrene using $\text{HRh}(\text{CO})(\text{PPh}_3)_3$ has been investigated in the temperature range 333–353 K. The effect of styrene and catalyst concentration, partial pressures of carbon monoxide and hydrogen on the rate of reaction has been investigated. The rate was found to be first order with respect to catalyst concentration and hydrogen partial pressure. The dependence of rate with CO, showed a typical substrate inhibited kinetics. The rate was found to be independent of styrene concentration. A rate equation has been proposed based on a mechanistic model and kinetic parameters evaluated. The activation energy was found to be $68.802 \text{ kJ mol}^{-1}$. © 1999 Elsevier Science B.V. All rights reserved.

Keywords: Kinetics; Hydroformylation; Styrene; Mechanistic model

1. Introduction

Hydroformylation of olefins is a well known synthetic tool for the preparation of a wide range of organic molecules of high commercial value [1]. It is also one of the largest scale applications of homogeneous catalysis in industry for the manufacture of Oxo alcohols. In recent years, new applications for high value added intermediate products for fine chemicals and pharmaceuticals are emerging [2]. An important example of the latter class is the hydroformylation of styrene or its derivatives to obtain aryl propionaldehydes, which on subsequent oxidation can give aryl propionic acid derivatives (e.g., Ibuprofen from *p*-isobutyl styrene substrate) [3–9]. The stoichiometric reaction is:



* Corresponding author

In earlier reports, hydroformylation of styrene using homogeneous Rh, Ru, Co and Pt–Sn, complex catalysts have been reported, in which the role of different ligands, and the activity/selectivity of the catalysts have been discussed [10–13]. In a very recent report, Ir–Pd, Ir–Hg, Ir–Cu, Ir–Tl, binuclear complexes containing a bifunctional ligand of the type Ph₂PPy as catalysts for hydroformylation of styrene have been reported [14].

Lazzaroni et al. [15] have studied the regioselectivity of styrene hydroformylation using Rh₄(CO)₁₂ as a catalyst precursor. Branched isomer, which is the major product in all cases, decreases with increase in temperature and decrease in CO or H₂ partial pressures. This has been explained with the help of deuterioformylation experiments which show that at room temperature, the formation of linear and branched alkyl intermediates from styrene and the catalytic complex is not reversible, whereas at higher temperatures mainly the branched alkyl intermediate gives back styrene via a β-hydride elimination, thus reducing the branched to linear isomer ratio.

Improvement in the rate of a low-pressure hydroformylation of styrene, with a catalytic species obtained by the substitution of Ph₂PPy in Wilkinson's catalyst, namely [HRh(CO)(PPh₃)₂(Ph₂PPy)], has been demonstrated by Gladiali et al. [16]. The use of ²H NMR spectroscopy to elucidate the catalytic pathway of the hydroformylation of styrene has been studied by Barretta et al. [17]. The difference in the behaviour of the metal-alkyl intermediates in the presence of Co₂(CO)₈ or Rh₄(CO)₁₂ has been discussed. With Co₂(CO)₈ as a catalyst precursor, the formation of a branched alkyl intermediate was found to be reversible, whereas, with Rh₄(CO)₁₂ catalyst this step was reversible only at higher temperature, mainly for the branched isomer. Wink et al. [18,19] have developed a highly active and regioselective cationic rhodium complex containing bis(dioxaphospholane) ligand. Aryl olefin substrates were hydroformylated with very high rates (> 3000 turnovers per Rh per hour) and high regioselectivity (> 92:8 for branched products). In another study, the influence of P–N bidentate ligands on the improvement of selectivity for rhodium catalysed hydroformylation has been reported [20]. Chan et al. [21] have reported the use of diphosphine rhodium complex catalyst with 1,2-bis[bis(pentafluorophenyl)-phosphino]ethane as a ligand, for a higher branched to linear isomer ratio.

Hydroformylation of olefins is an example of a complex reaction system as simultaneous dissolution of two or more gases, followed by a catalytic reaction is involved. A knowledge of the kinetics and development of rate equations is important in understanding the mechanistic features of such complex reactions. Kinetic modelling of hydroformylation of olefins has been studied extensively for a variety of substrates (e.g., vinyl acetate, allyl alcohol, hexene, decene and dodecene) [22–25]. Kinetics of hydroformylation of styrene using Rh-1,2,5-triphenyl-1*H*-phosphole system is reported by Bergouniou et al. [26], in which a first order dependence of the rate with catalyst, styrene and hydrogen and a negative first order with respect to CO has been observed. In all these studies, empirical rate equations were used to represent the kinetics. It will be more appropriate to study the kinetics based on a mechanistic model derived using a molecular level description of the catalytic cycle. Such an approach to kinetic modeling of hydroformylation of 1-decene using HRh(CO)(PPh₃)₃ has been reported by Divekar et al. [27]. However, in this study, only the dependence of the rate on CO has been explained. In a recent paper, by van Leeuwen, kinetics of hydroformylation of octene, cyclohexene and styrene has been studied using rhodium-[tris(2-*tert*-butyl-4-menthylphenyl) phosphite] catalyst [28]. The rate data for 1-octene have been explained using a rate equation derived assuming the oxidative addition of hydrogen to acylrhodium intermediate complex as the rate determining step. For cyclohexene hydroformylation, addition of cyclohexene to the starting rhodium hydride complex is considered as a rate determining step. Kinetics of hydroformylation of styrene was found to be more complex and the rate expression for octene or cyclohexene was not found to be

suitable for this system [28]. None of these studies have attempted evaluation of rate parameters using a mechanistic model.

In this paper, the kinetics of hydroformylation of styrene using the homogeneous $\text{HRh}(\text{CO})(\text{PPh}_3)_3$ complex catalyst has been studied and a detailed analysis of the rate equation based on mechanistic model is discussed. The dependence of rate on catalyst and styrene concentrations, and partial pressures of CO and H_2 on the rate of hydroformylation has been studied in the temperature range of 333 K to 353 K, and the kinetic parameters evaluated.

2. Experimental

2.1. Materials

Rhodium trichloride ($\text{RhCl}_3 \cdot 3\text{H}_2\text{O}$) [Aldrich, USA], triphenyl phosphine and styrene [Fluka, Switzerland] were used as received without further purification. Hydrogen [Indian Oxygen, Bombay] and carbon monoxide [$> 99.8\%$ pure, Matheson Gas, USA] were used directly from cylinders. The syngas mixture [$(\text{H}_2 + \text{CO})$ with 1:1 ratio] was prepared by mixing H_2 and CO in a reservoir vessel. The solvents, toluene and ethanol were freshly distilled and dried prior to use. The catalyst, $\text{HRh}(\text{CO})(\text{PPh}_3)_3$, was prepared by the procedure given by Evans et al. [29].

2.2. Experimental setup

All the hydroformylation experiments were carried out in a 50-ml microreactor, supplied by Parr Instrument, USA. The reactor was provided with arrangements for sampling of liquid and gaseous contents, automatic temperature control and variable stirrer speed. The reactor was designed for a working pressure of 2000 psi and temperature up to 250°C . A safety rupture disk was also fitted to the reactor. The consumption of CO and H_2 at a constant pressure was monitored by observation of the pressure drop in the gas reservoir, from which $(\text{CO} + \text{H}_2)$ mixture was supplied through a constant pressure regulator at 1:1 ratio. The pressure in the reservoir was recorded using a pressure transducer to follow the consumption of $\text{CO} + \text{H}_2$ as a function of time. A schematic diagram of the experiment setup is shown in Fig. 1.

2.3. Experimental procedure

In a typical experiment, known quantities of the catalyst and styrene, along with the solvent were charged into the autoclave and the reactor was flushed with nitrogen. The contents were then flushed with a mixture of CO and H_2 and heated to the desired temperature. A mixture of CO and H_2 , in the required ratio, was introduced into the autoclave, a sample of liquid withdrawn, and the reaction started by switching the stirrer on. The reaction was then continued at a constant pressure by supply of $\text{CO} + \text{H}_2$ (1:1) from the reservoir vessel. Since the major products formed were isomeric aldehydes, supply of $\text{CO} + \text{H}_2$ at a ratio of 1:1 (as per stoichiometry) was adequate to maintain a constant composition of CO and H_2 in the autoclave, as introduced in the beginning. This was confirmed in a few cases by analysis of the CO content in the gas phase at the end of the reaction. All the reactions for kinetic studies were carried out for short durations such that the conversion in the liquid phase was minimum, to ensure differential conditions. In each kinetic run, samples were

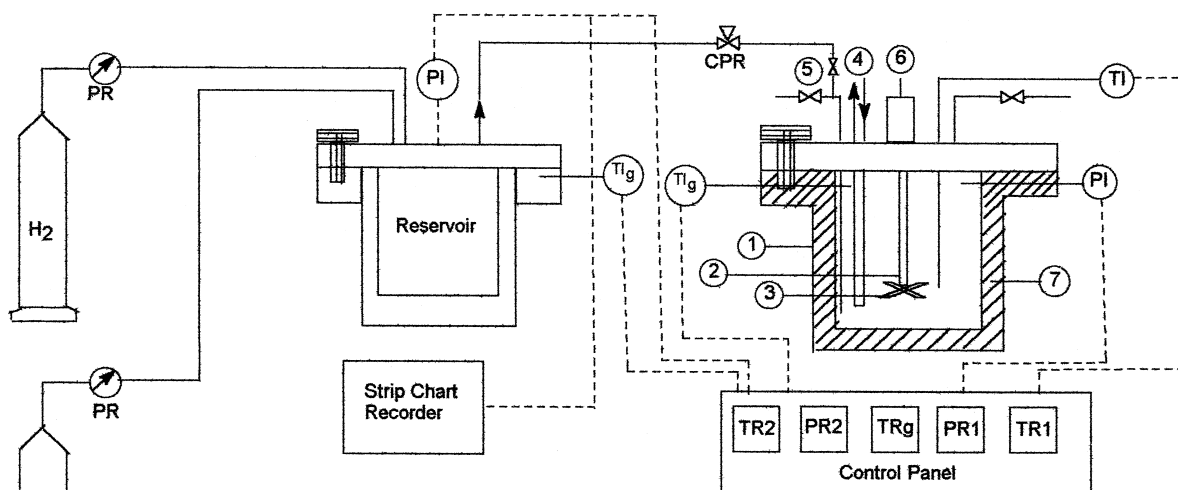


Fig. 1. Schematic of the reactor setup. (1) Reactor, (2) Stirrer shaft, (3) Impeller, (4) Cooling water, (5) Sampling valve, (6) Magnetic stirrer, (7) Furnace, TI: Thermocouple, PI: Pressure Transducer, CPR: Constant Pressure Regulator, PR: Pressure Regulator, TRI: Reactor Temperature Indicator, TRG: Gas Temperature Indicator, PRI: Reactor Pressure Indicator, PR2: Reservoir Pressure Indicator, TR2: Reservoir Temperature Indicator.

withdrawn at regular intervals of time and analysed for reactants and products in order to check the material balance. The reproducibility of the experiments was found to be in a range of 5–7%. Following this procedure, the effect of the catalyst and styrene concentrations, partial pressure of H_2 and CO and temperature on the rate of hydroformylation was studied.

The analysis of reactants and products was carried out by a gas chromatographic method on a 10% OV-17 column of 8-ft long. For this purpose, an HP5840 gas chromatography was used. The two aldehyde products, 2-phenyl propionaldehyde (2ppd) and 3-phenyl propionaldehyde (3ppd) were identified by GCMS.

3. Results and discussion

The main objective of this work was to investigate the kinetics of hydroformylation of styrene using the homogeneous $HRhCO(PPh_3)_3$ complex catalyst. It was therefore thought necessary to first check the material balance and reproducibility of the experiments. For this purpose, a few experiments were carried out in which the amount of styrene consumed, products formed, and $CO + H_2$ consumed were compared for experiments with high conversion of styrene. A typical concentration-time profile is shown in Fig. 2. In general, it was observed that the material balance of CO, H_2 and styrene consumed was consistent with the amount of total aldehyde products formed. Also, in the range of conditions covered in this work, the only products formed were 2-phenyl propionaldehyde and 3-phenyl propionaldehyde. No hydrogenation or isomerisation products were observed. In order

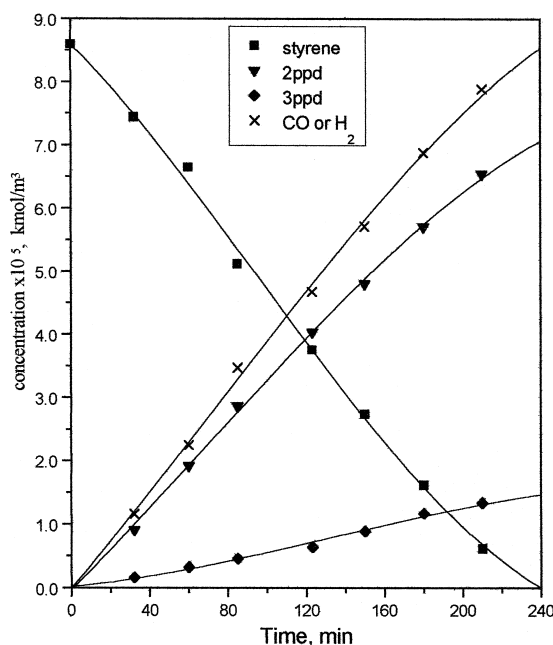


Fig. 2. Concentration-time profile of a batch reactor: Styrene hydroformylation. Reaction conditions: styrene: 3.45 kmol m^{-3} ; catalyst: 1.01 kmol m^{-3} ; H_2 partial pressure: 2.04 MPa ; CO partial pressure: 2.04 MPa ; agitation speed: 15 Hz ; solvent: toluene; total volume: $2.5 \times 10^{-5} \text{ m}^3$, reaction time: 120 min .

to study the kinetics, it was important to ensure that reactions were carried out under kinetic regime. The experiments at different agitation speeds showed that the rate of the reaction was independent of the agitation speed beyond 400 rpm , indicating kinetic regime. All the reactions were therefore carried out at an agitation speed of 900 rpm (15 Hz) to ensure kinetic regime.

3.1. Solubility data

For interpretation of kinetic data, knowledge of the concentration of the gaseous reactants in the reaction medium is essential. The solubility of CO and H_2 in toluene, styrene and styrene/toluene mixtures was determined experimentally at 333 K , 343 K and 353 K , using a method described earlier [30]. The results are presented as Henry's law constant in Tables 1 and 2, which indicate that the

Table 1
Henry's constants of CO in toluene, styrene, and toluene–styrene mixture

Gas, solvent	H , $\text{MPa m}^3 \text{ kmol}^{-1}$ at 333 K		H , $\text{MPa m}^3 \text{ kmol}^{-1}$ at 343 K		H , $\text{MPa m}^3 \text{ kmol}^{-1}$ at 353 K	
	Observed	Predicted	Observed	Predicted	Observed	Predicted
CO in toluene	11.90	11.86	11.70	11.73	11.53	11.59
CO in 10% styrene in toluene	12.01	12.02	11.85	11.87	11.70	11.72
CO in 20% styrene in toluene	12.20	12.16	11.99	12.01	11.87	11.85
CO in 40% styrene in toluene	12.82	12.47	12.41	12.29	12.41	12.11
CO in 80% styrene in toluene	13.10	13.13	12.93	12.91	12.72	12.69
CO in styrene	13.60	13.47	13.32	13.22	13.10	12.98

Table 2

Henry's constants of hydrogen in toluene, styrene, and toluene–styrene mixture

Gas, solvent	H , MPa m ³ kmol ⁻¹ at 333 K		H , MPa m ³ kmol ⁻¹ at 343 K		H , MPa m ³ kmol ⁻¹ at 353 K	
	Observed	Predicted	Observed	Predicted	Observed	Predicted
H ₂ in toluene	29.30	29.27	28.10	28.06	26.80	26.96
H ₂ in 10% styrene in toluene	29.58	29.61	28.40	28.36	27.22	27.24
H ₂ in 20% styrene in toluene	30.01	29.98	28.65	28.70	27.50	27.54
H ₂ in 40% styrene in toluene	31.60	31.55	30.10	30.12	28.58	28.82
H ₂ in 80% styrene in toluene	32.42	32.39	30.92	30.89	29.55	29.52
H ₂ in styrene	33.22	33.23	31.83	31.65	30.50	30.20

increase in styrene concentration in toluene decreases the solubility of both CO and H₂ only marginally (5–7%).

The Henry's constant for carbon monoxide in toluene and styrene were also calculated using the correlation proposed by Reid and Prausnitz [31] based on the theory of regular solution. The correlation used was:

$$-\ln \chi_A = \ln(f_A^L/f_A) + \left\{ \phi_S V_A (\delta_S - \delta_A)^2 / RT \right\} \quad (1)$$

The use of Eq. (1) requires a knowledge of three parameters of the solute viz.: fugacity of hypothetical liquid, f_A^L (atm), solubility parameter δ , (J m⁻³)^{1/2} and molar volume V_A , (m³ mol⁻¹). The fugacity of hypothetical liquid solute (f_A^L) depends upon the critical temperature and critical pressure of the gases and was calculated from a correlation between fugacity and temperature, as reported by Yen and McKetta [32]. The regular solution theory also states that the solubility parameters for gas (δ_A) and molar volume of solutes are independent of temperature and were obtained from the work of Prausnitz and Shair [33] (6.4×10^3 J^{0.5} m^{-1.5} for CO and 7.835×10^3 J^{0.5} m^{-1.5} for H₂). The solubility parameter (δ_S) for toluene and styrene was calculated from the heat of vaporisation as proposed by Hildebrand and Scott [34]

$$\delta_S = (\Delta H - RT/V_A)^{1/2} \quad (2)$$

The solubility values of CO and H₂ in pure toluene and pure styrene were further used for calculating the solubilities of these gases in a mixture of solvents (toluene/styrene) by using the method described by Hildebrand and Scott [34], and given by following expression:

$$(\ln \chi_A)_{\text{mix}} = \phi_1 \ln(\chi_{A1}) + \phi_2 \ln(\chi_{A2}) - V_A \beta_{12} \phi_1 \phi_2 \quad (3)$$

where $\beta_{12} = (\delta_{S1} - \delta_{S2})^2 / RT$; X_{A1} , X_{A2} and ϕ_1 , ϕ_2 are the mole fraction of a gas in pure toluene and styrene and the volume fraction of solvent, respectively. δ_{S1} and δ_{S2} are the solubility parameters for toluene and styrene. The results predicted for pure toluene, styrene and styrene/toluene mixtures were found to be in good agreement with the experimental values (within $\pm 3\%$) and are shown in Tables 1 and 2. These data were used in the calculation of the concentrations of dissolved CO and H₂ in the liquid medium for interpretation of the kinetics.

3.2. Initial rate data

In order to study the kinetics of the hydroformylation of styrene using HRh(CO)(PPh₃)₃ in toluene, several experiments were carried out in the range of conditions as shown in Table 3. The initial rates

Table 3

Range of conditions for kinetic study

Concentration of catalyst (kmol m^{-3})	0.131–1.01
Concentration of styrene (kmol m^{-3})	0.92–6.89
Partial pressure of hydrogen (MPa)	1.03–4.12
Partial pressure of carbon monoxide (MPa)	0.3–4.12
Temperature (K)	333–353
Solvent	toluene
Reaction volume (m^3)	2.5×10^{-5}

of hydroformylation were calculated from observed data on the consumption of $\text{CO} + \text{H}_2$ as function of time. The rate of hydroformylation was calculated from the slope of CO or H_2 vs. time plots. These were essentially initial rates of reaction, calculated under low conversion ($< 10\%$) conditions. The results showing the dependence of the rates on different parameters and a kinetic model are discussed in the following sections.

The rate of hydroformylation of styrene was observed to be linearly dependent with respect to the catalyst precursor $[\text{HRh}(\text{CO})(\text{PPh}_3)_3]$ concentration and hydrogen partial pressure. These results are shown in Figs. 3 and 4. A first-order dependency on hydrogen indicates that the oxidative addition of H_2 to the acylrhodium intermediate species is the rate-determining step. Similarly, the first order dependence with respect to catalyst is consistent with increase in the active Rh species concentration with increase in the catalyst precursor concentration.

The rate of hydroformylation of styrene vs. partial pressure of CO plot shows a typical substrate inhibited kinetics. The results are shown in Fig. 5 for all the temperatures studied. As per the mechanism of hydroformylation proposed by Evans et al. [29] (see Fig. 6), the inhibition of the rate of hydroformylation with increase in partial pressure of CO is due to the side reactions leading to the formation of inactive dicarbonyl $[(\text{RCO})\text{Rh}(\text{CO})_2(\text{PPh}_3)]$ and tricarbonyl $[(\text{RCO})\text{Rh}(\text{CO})_3(\text{PPh}_3)]$, rhodium species. With increase in CO pressure, the concentration of these species is expected to

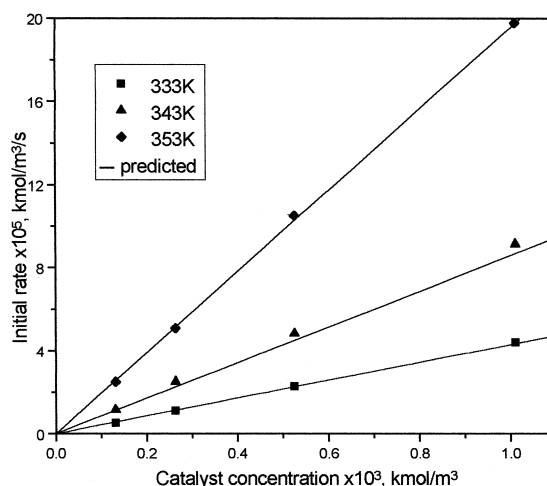


Fig. 3. Effect of catalyst concentration on the rate of hydroformylation. Reaction conditions: styrene: 3.45 kmol m^{-3} ; H_2 partial pressure: 2.04 MPa; CO partial pressure: 2.04 MPa; agitation speed: 15 Hz; solvent: toluene; total volume: $2.5 \times 10^{-5} \text{ m}^3$, reaction time: 120 min.

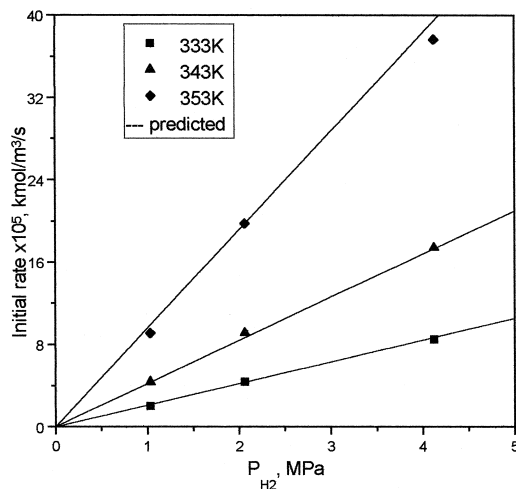


Fig. 4. Effect of hydrogen partial pressure on rate of hydroformylation. Reaction conditions: styrene: 3.45 kmol m^{-3} ; catalyst: 1.01 kmol m^{-3} ; CO partial pressure: 2.04 MPa ; agitation speed: 15 Hz ; solvent: toluene; total volume: $2.5 \times 10^{-5} \text{ m}^3$, reaction time: 120 min .

increase, reducing the active species concentration and hence the rate of reaction. The observation of a negative order dependence with CO partial pressure was also reported for other olefinic substrates. [22–28].

The rate of hydroformylation was found to be zero order with respect to styrene in the range of concentrations (0.92 to 6.89 kmol m^{-3}) studied. The results are shown in Fig. 7. Unlike the previous reports [22,23] wherein the kinetics was found to be first order tending to zero order with 1-dodecene,

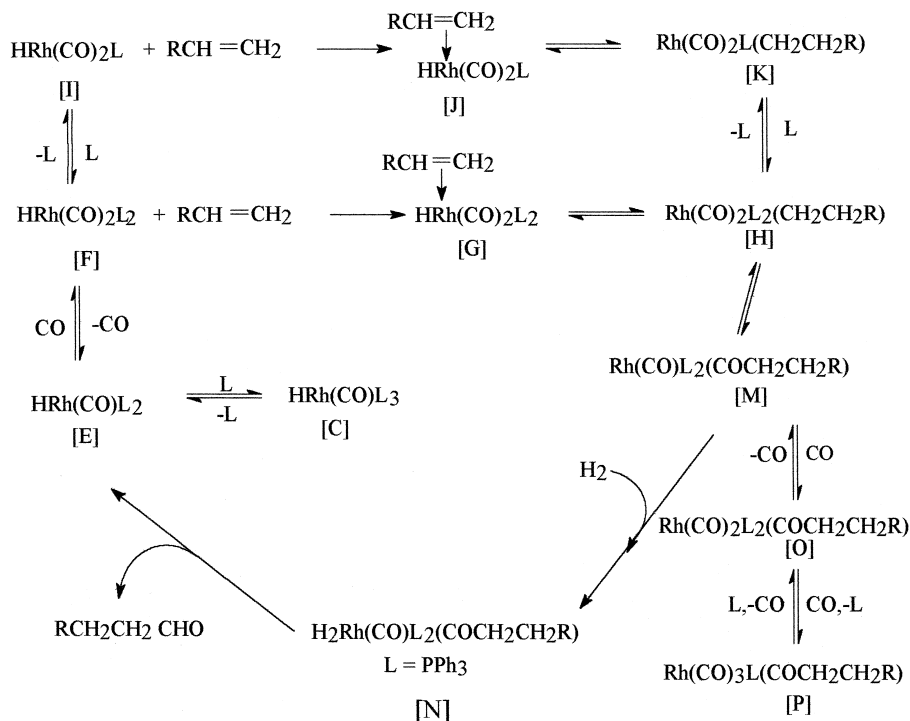


Fig. 5. Mechanism of hydroformylation of olefins.

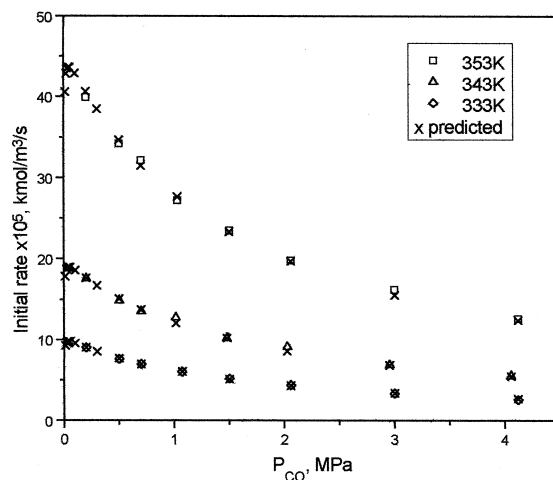


Fig. 6. Effect of carbon monoxide partial pressure on rate of hydroformylation. Reaction conditions: styrene: 3.45 kmol m^{-3} ; catalyst: 1.01 mol m^{-3} ; CO partial pressure: 2.04 MPa ; agitation speed: 15 Hz ; solvent: toluene; total volume: $2.5 \times 10^{-5} \text{ m}^3$, reaction time: 120 min .

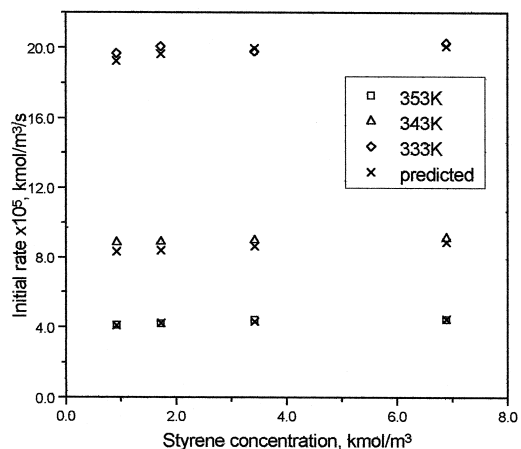


Fig. 7. Effect of styrene concentration on rate of hydroformylation. Reaction conditions: catalyst: 1.01 kmol m^{-3} ; H_2 partial pressure: 2.04 MPa ; CO partial pressure: 2.04 MPa ; agitation speed: 15 Hz ; solvent: toluene; total volume: $2.5 \times 10^{-5} \text{ m}^3$, reaction time: 120 min .

and a negative order in case of allyl alcohol, here the rate was found to be independent of styrene concentration. According to the simplified reaction scheme (step 2), the addition of olefin to form the olefin-Rh complex is an equilibrium reaction. The equilibrium may be attained even at lower concentration of styrene leading to a zero order dependence. Zero order dependence of styrene was also observed by Lazzaroni et al. [35] with $\text{Rh}_4(\text{CO})_{12}$ catalyst at 90°C and 180 bar total pressure of $(\text{CO} + \text{H}_2)$. However in some reports, a substrate inhibited kinetics with respect olefin has been observed [25].

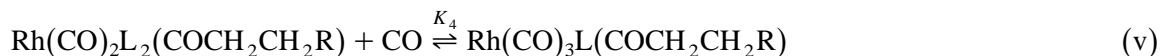
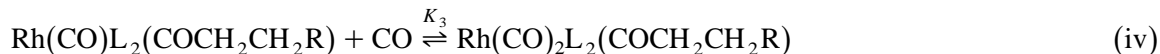
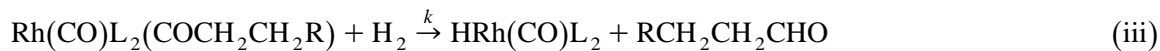
Table 4

Rate constants evaluated from the rate model

Temperature	$k, \text{ m}^3 \text{ kmol}^{-1} \text{ s}^{-1}$	$K_1, \text{ m}^3 \text{ kmol}^{-1}$	$K_2, \text{ m}^3 \text{ kmol}^{-1}$	$K_3, \text{ m}^3 \text{ kmol}^{-1}$	$K_4, \text{ m}^3 \text{ kmol}^{-1}$
333	1.61248	469.11	7.548	8.7372	0.05855
343	3.0482	404.5	7.515	8.539	0.05513
353	6.5915	337.695	7.4765	8.3575	0.05356

3.3. Kinetic model

In order to derive a rate equation, the catalytic cycle (Fig. 5) described by Evans et al. [29] was considered. The elementary steps involved in the catalytic cycle, can be simplified as shown below:



Assuming that the oxidative addition of hydrogen to the acylrhodium species is rate determining, the following rate equation can be derived.

$$R = \frac{kK_1K_2ABCD}{1 + K_1B + K_1K_2BD + K_1K_2K_3B^2D + K_1K_2K_3K_4B^3D} \quad (4)$$

where K_1 , K_2 , K_3 , K_4 are the equilibrium constants of various steps given above, and k is the reaction rate constant. In order to estimate the rate parameters, a non-linear least square regression analysis was used to fit the rate data using Eq. (4) and obtain the best fit parameters. For this purpose, an optimization program based on a Marquart's method [36] was used. The model parameters were estimated by minimizing the objective function ϕ_{\min} , defined as:

$$\phi_{\min} = \sum_{i=1}^n [R_{A_i} - R'_{A_i}]^2 \quad (5)$$

where R_{A_i} and R'_{A_i} are the observed and predicted rates, respectively and n is the number of points.

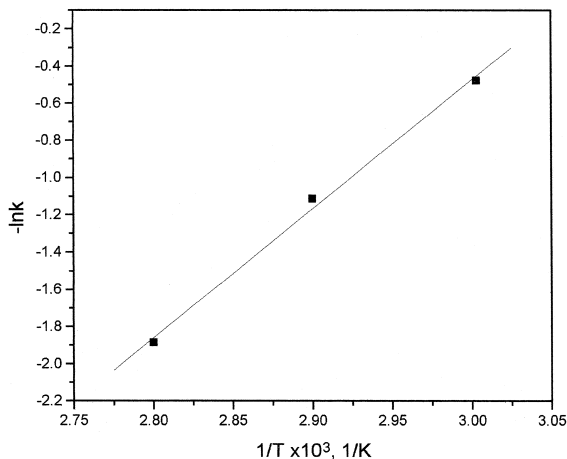


Fig. 8. Temperature dependence of rate constant.

The model was further subjected to residual analysis, in which the relative residuals (RR) of the model predictions were considered. (RR) is defined as

$$\text{RR} = \frac{R_{A_i} - R'_{A_i}}{R_{A_i}} \times 100 \quad (6)$$

The RR values for the model were scattered and did not show any regular trends with respect to any parameter, thus confirming the validity of the model. The error between the predicted and observed rate data was found to be $\pm 5\%$. The rate and equilibrium parameters determined for different temperatures are presented in Table 4. From the temperature dependence of the rate constants (Fig. 8), the activation energy was found to be $68.802 \text{ kJ mol}^{-1}$.

4. Conclusion

Kinetics of hydroformylation of styrene using a homogeneous $\text{HRh}(\text{CO})(\text{PPh}_3)_3$ was studied in a batch pressure reactor in a temperature range of 333–353 K. The reaction was found to be first order with respect to catalyst and H_2 partial pressure. The rate vs. partial pressure of CO showed a negative order dependence with CO indicating a substrate inhibited kinetics. Change in styrene concentration showed no effect on the rate of hydroformylation. A rate equation has been derived using a catalytic cycle based on molecular level description of elementary steps and assuming oxidative addition of hydrogen to acylrhodium intermediate as the rate determining step. The kinetic parameters were estimated using a non-linear regression analysis. The mechanistic model proposed was found to predict the data within $\pm 5\%$ error at all temperatures. The activation energy was found to be $68.802 \text{ kJ mol}^{-1}$.

5. Nomenclature

A	Concentration of H_2 in the reaction mixture, kmol m^{-3}
B	Concentration of CO in the reaction mixture, kmol m^{-3}
C	Catalyst concentration, kmol m^{-3}
D	Styrene concentration, kmol m^{-3}
f_A	Fugacity of pure gas at atmospheric pressure, MPa
f_A^L	Fugacity of hypothetical liquid solute at atmospheric pressure, MPa
k	Reaction rate constant, $\text{m}^3 \text{ kmol}^{-1} \text{ s}^{-1}$
K_1, K_2, K_3, K_4	Equilibrium constants for the elementary steps i, ii, iv, and v, respectively in the catalytic cycle, $\text{m}^3 \text{ kmol}^{-1}$
R_{A_i}	Observed rate, $\text{kmol m}^{-3} \text{ s}^{-1}$
R'_{A_i}	Predicted rate, $\text{kmol m}^{-3} \text{ s}^{-1}$
R	Gas constant, $\text{J K}^{-1} \text{ mol}^{-1}$
T	Temperature, K
δ_A	Solubility parameter for the solute gas, $(\text{J m}^{-3})^{1/2}$
χ_A	Mole fraction of gas A
ϕ_S	Volume fraction of solvent

ν_A	Molar volume of gas A, $\text{m}^3 \text{mol}^{-1}$
δ_S	Solubility parameter for solvent, $(\text{J m}^{-3})^{1/2}$
δ_A	Solubility parameter of solute $(\text{J m}^{-3})^{1/2}$
β_{12}	$(\delta_{S1} - \delta_{S2})^2 / RT$
$\chi_{A,\text{mix}}$	Mole fraction of gas in the solvent mixture
χ_{A1}	Mole fraction of gas in pure styrene
χ_{A2}	Mole fraction of gas in pure toluene

References

- [1] B. Cornils, W.A. Herrmann, *Applied Homogeneous Catalysis with Organometallic Compounds*, Vol. 1, Chap. 2, VCH Publ., 1996, p. 303.
- [2] G.W. Parshall, W.A. Nugent, *CHEMTECH* (1988) 184.
- [3] T. Shimasaki, Y. Otsuka, H. Kondo, *Jpn. Kokai* 79 (1979) 123–336.
- [4] Y. Fujimory, *Jpn. Kokai* 78,82,740, 1978.
- [5] K. Takeuchi, Y. Sugi, T. Matsuzaki, *Chem. Ind.* (1985) 446.
- [6] M. Miekus, F. Joo, H. Alper, *Organometallics* 1 (1982) 775.
- [7] W.A. Nugent, R.J. McKinner, *J. Org. Chem.* 50 (1985) 5370.
- [8] M. Arakawa (Nado Kenkyusho) *JP* 77,97,930 (1977).
- [9] J.P. Rieu, A. Boucherle, H. Cousse, G. Mouzin, *Tetrahedron* 42 (1986) 4095.
- [10] Cerriotti, L. Goulaschelli, G. Longoni, M.C. Malatesta, O.J. Strumolo, *J. Mol. Catal.* 24 (1984) 309.
- [11] G. Muller, D. Saniz, J. Sales, *J. Mol. Catal.* 63 (1990) 173.
- [12] T. Hayashi, Z. Huigue, T. Sakakura, M. Tanaka, *J. Organomet. Chem.* 352 (1988) 373.
- [13] D. Neibecker, R. Reau, *J. Org. Chem.* 54 (1989) 5208.
- [14] G. Francio, R. Scopelliti, C.G. Arena, G. Bruno, D. Drommi, F. Faraone, *Organometallics* 17 (1988) 338.
- [15] R. Lazzaroni, A. Raffaelli, R. Settambolo, S. Bertozzi, G. Vitulli, *J. Mol. Catal.* 50 (1989) 1.
- [16] S. Gladiali, L. Pinna, C.G. Arena, E. Rotondo, F. Faraone, *J. Mol. Catal.* 66 (1991) 183.
- [17] G.U. Barretta, R. Lazzaroni, R. Settambolo, P. Salvadori, *J. Organomet. Chem.* 417 (1991) 111.
- [18] D.J. Wink, T.J. Kwok, A. Yee, *Inorg. Chem.* 29 (1990) 5006.
- [19] T.J. Kwok, D.J. Wink, *Organometallics* 12 (1993) 1954.
- [20] C.A. Gnim, I. Amer, *J. Mol. Catal.* 85 (1993) L275.
- [21] A.S.C. Chan, C.C. Pai, T.K. Yang, S.M. Chen, *J. Chem. Soc. Chem. Commun.* (1995) 2031.
- [22] R.M. Deshpande, R.V. Chaudhari, *J. Catal.* 115 (1989) 326.
- [23] B.M. Bhanage, S.S. Divekar, R.M. Deshpande, R.V. Chaudhari, *J. Mol. Catal. A: Chem.* 115 (1997) 247.
- [24] R.M. Deshpande, R.V. Chaudhari, *Ind. Eng. Chem. Res.* 27 (1988, 1996).
- [25] R.M. Deshpande, R.V. Chaudhari, *J. Mol. Catal.* 57 (1989) 177.
- [26] C. Bergouniou, D. Neibecker, R. Rieu, *Bull. Soc. Chim. Fr.* 132 (8) (1995) 815.
- [27] S.S. Divekar, R.M. Deshpande, R.V. Chaudhari, *Catal. Lett.* 21 (1993) 191.
- [28] A. Van Rooy, E.N. Oriji, P.C.J. Kamer, P.W.N.M. Van Leeuwen, *Organometallics* 14 (1995) 3.
- [29] D. Evans, J. Osborn, G. Wilkinson, *J. Chem. Soc. A* (1968) 3133.
- [30] P. Purvanto, R.M. Deshpande, R.V. Chaudhari, H. Delmas, *J. Chem. Eng. Data* 41 (1996) 1414.
- [31] R.C. Reid, J.M. Prausnitz, *The Properties of Gases and Liquids*, McGraw-Hill, 1987.
- [32] L.C. Yen, J.J. McKetta, *AIChE J.* 8 (4) (1962) 501.
- [33] J.M. Prausnitz, F.H. Shair, *AIChE J.* 7 (1961) 682.
- [34] J.H. Hildebrand, R.L. Scott, *Solubility of electrolytes and non-electrolytes*, American Chemical Society 424 (1948) 9.
- [35] R. Lazzaroni, P. Pertici, S. Bertozzi, G. Fabrizi, *J. Mol. Catal.* 58 (1990) 75.
- [36] K. Radhakrishnan, P.A. Ramachandran, P.H. Brahme, R.V. Chaudhari, *J. Chem. Eng. Data* 28 (1983) 1–4.